Elastic nucleon-nucleon cross section in nuclear matter at finite temperature

A. Schnell,[1] G. Röpke,[1] U. Lombardo,[2,3] and H.-J. Schulze[4]
[1]AG Vielteilchenphysik, FB Physik, Universität Rostock, D-18051 Rostock, Germany
[2]INFN-LNS, 44 Via S. Sofia, I-95123 Catania, Italy
[3]Dipartimento di Fisica, 57 Corso Italia, I-95129 Catania, Italy
[4]INFN, Sezione di Catania, 57 Corso Italia, I-95129 Catania, Italy
(Received 2 October 1997)

We calculate the elastic nucleon-nucleon cross section in symmetric nuclear matter at finite temperature by determining the nonrelativistic in-medium scattering matrix with a realistic nucleon-nucleon potential. We define average in-medium cross sections depending on density and temperature and provide simple parametrizations for the use in numerical simulations of heavy-ion collisions. The effect of hole-hole propagation in the nuclear medium is found to be small. [S0556-2813(98)01802-0]

PACS number(s): 25.70.−z, 21.30.Fe, 13.75.Cs, 21.65.+f

The description of nuclear matter as function of temperature and density, i.e., the nuclear equation of state (EOS), is of high interest. A wide variety of heavy-ion experiments is aimed at knowledge of the behavior of the expanding, hot, and dense hadron gas. In heavy-ion collisions (HIC's) at bombarding energies up to 250 MeV/nucleon, nucleons are the relevant degrees of freedom and a nonrelativistic approach is assumed to be a good approximation. Recent experimental results concerning the caloric curve of nuclear matter [1], the formation of intermediate mass fragments [2], and the occurrence of collective flow [3] probe various aspects of the EOS.

A theoretical description of heavy-ion collisions has to face many difficulties since the process is extremely far from equilibrium. Transport-model equations such as the Boltzmann-Uehling-Uhlenbeck (BUU) model are a well-established method to simulate the space-time evolution of such collisions [4–10]. A basic ingredient for these calculations is the elastic nucleon-nucleon scattering cross section [11]. In order to describe the scattering process in the hot and dense hadron gas, medium modifications of the free cross section have to be taken into account.

It is the purpose of this article to extend our previous publication [12], where we performed a zero temperature calculation within Brueckner theory, to give an estimate of the *temperature* and density behavior of the in-medium nucleon-nucleon cross section. Besides the extension to finite temperature, we investigate also the effect of including hole-hole scattering processes in the in-medium interaction, i.e., the transition from the Brueckner G matrix to the thermodynamic T matrix (see also, e.g., Ref. [13]).

We use a separable version of a realistic nucleon-nucleon interaction [Bonn relativistic momentum space one-boson-exchange (OBEPQ) potential [14]], as given by Plessas *et al.* [15], and restrict to intermediate scattering energies $E \lesssim 400$ MeV, where inelastic channels (Δ resonance) are not yet open.

As for a detailed derivation of the in-medium nucleon-nucleon cross section in the G and T matrix approach we refer the reader to previous articles [12,16,17]. Here, we only sketch out the basic formulas, starting from the definition of the total cross section in terms of the G or T matrix elements (t denoting total isospin),

$$\sigma_t(k,P,W,\rho,T)=\frac{4\pi}{k^2}\frac{N^2(k,P)}{(2s_1+1)(2s_2+1)}\sum_{S,J,L,L'}(2J+1)\times|G_{LL'}^{tSJ}(k,k,P,W)|^2, \tag{1}$$

which is a function of the relative momentum k, the total momentum P, and the energy W of the nucleon pair, as well as the nucleon density ρ and temperature T. The in-medium scattering matrix is the solution of the integral equation

$$G[W]=V+\sum_{p,p'}V|pp'\rangle\frac{Q}{W-E+i\epsilon}\langle pp'|G[W], \tag{2}$$

where $E=e(p)+e(p')$ is the energy of the intermediate two-nucleon state. The single-particle energies are determined along with the G matrix in a self-consistent scheme according to the equation

$$e(p)=\frac{p^2}{2m}+U(p)=\frac{p^2}{2m}+\mathrm{Re}\sum_{p'}f(p')\langle pp'|\times G[e(p)+e(p')]|pp'\rangle_A, \tag{3}$$

where $f(p)=\{1+\exp[e(p)-\mu]/T\}^{-1}$ denotes the Fermi distribution for a given temperature and chemical potential μ.

The angle-averaged Pauli operator Q in Eq. (2) restricts the intermediate propagation to either only particle-particle states (G matrix) or including hole-hole states (T matrix), $Q_G=Q_{\rm pp}$, $Q_T=Q_{\rm pp}-Q_{\rm hh}$, with

$$Q_{\rm pp}(k,P)=\int\frac{d\Omega}{4\pi}[1-f(\boldsymbol{P}/2+\boldsymbol{k})][1-f(\boldsymbol{P}/2-\boldsymbol{k})], \tag{4a}$$

$$Q_{\rm hh}(k,P)=\int\frac{d\Omega}{4\pi}f(\boldsymbol{P}/2+\boldsymbol{k})f(\boldsymbol{P}/2-\boldsymbol{k}). \tag{4b}$$

(Ω denotes the solid angle spanned by $\boldsymbol{k}$.) We emphasize, however, that for the self-consistent determination of the single-particle energies [Eqs. (2) and (3)] we always use the Brueckner-Hartree-Fock prescription [18] and do not consider the hole-hole contributions. Including these leads to a

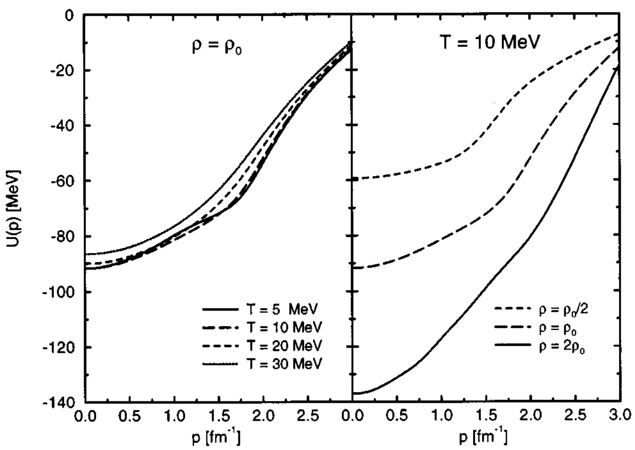

FIG. 1. Single-particle potentials as a function of the momentum p at fixed density $\rho = \rho_0$ and various temperatures (left) and at fixed temperature $T = 10$ MeV for various values of the density (right).

pairing singularity in the T matrix below a certain critical temperature in accordance with the Thouless criterion [17]. This effect prevents a self-consistent calculation of the single-particle energies in the T matrix approach at low temperature.

The second ingredient of Eq. (1) is the generalized density of states, N, defined as

$$N(k,P) = \left[\frac{\partial E(k,P)}{\partial k}\right]^{-1}, \tag{5}$$

with the angle-averaged two-particle energy

$$E(k,P) = \int \frac{d\Omega}{4\pi}[e(\boldsymbol{P}/2+\boldsymbol{k}) + e(\boldsymbol{P}/2-\boldsymbol{k})]. \tag{6}$$

It is related to the two-nucleon effective mass [12] via

$$N(k,P) = \frac{M^*(k,P)}{2k}. \tag{7}$$

In Ref. [12] it was demonstrated that in fact this quantity dominates the in-medium modification (suppression) of the cross section by counteracting a weaker enhancement of the in-medium G matrix elements.

Another important result of Ref. [12] was the fact that, as far as in-medium effects are concerned, there is very little difference between the proton-proton and the proton-neutron cross sections. In the present article we can therefore restrict ourselves to the isospin-averaged nucleon-nucleon cross section

$$\sigma_{NN} = \frac{1}{2}[\sigma_{pp} + \sigma_{pn}] = \frac{1}{4}[\sigma_0 + 3\sigma_1]. \tag{8}$$

For the calculation of the in-medium cross section the self-consistent determination of the single-particle energies (3) has to be performed at each point (ρ,T) of the density-temperature plane. In Fig. 1 we display the real part of the nucleon on-shell self-energy (single-particle potential) as a function of the momentum for different values of the temperature and density ($\rho_0 = 0.17$ fm^{-3}, saturation density of nuclear matter). One notes a rather weak temperature dependence, although the wiggle in the vicinity of the Fermi momentum, which is still present at the lowest temperature (5 MeV) and leads to a considerable enhancement of the effective mass near k_F, is wiped out with increasing temperature [18]. This result is in accordance with the calculations of Lejeune *et al.* [19].

In previous publications we reported extensively on the behavior of the cross section, Eq. (1), as function of temperature, density, and total momentum [17]. In particular, we showed that a singularity in the cross section occurs for low temperatures as a precursor effect of the onset of superfluidity. This phenomenon made it difficult to give an overall estimate of the cross section in a large range of temperature and density. However, during the evolution of a HIC's before the freeze-out, the values of density, temperature, and total momentum of single pairs are such that the superfluid can hardly occur. Moreover, the application to transport-model simulations does not demand keeping the full dependence of the cross section upon all variables, but a suitable averaging procedure can be applied much the same as has been done for zero temperature in Ref. [12]. In accordance with the loss term of the collisional integral in the Boltzmann equation we define

$$\langle\sigma\rangle(p_1) = \frac{\int d^3p_2 f(p_2) Q_{\rm pp}(k,P)\sigma_{NN}(k,P)/N(k,P)}{\int d^3p_2 f(p_2)/N(k,P)}, \tag{9}$$

with $\boldsymbol{P} = \boldsymbol{p}_1 + \boldsymbol{p}_2$ and $\boldsymbol{k} = (\boldsymbol{p}_1 - \boldsymbol{p}_2)/2$. Then, we end up with an average cross section that depends besides on an average scattering energy $E := p_1^2/2m$ only on temperature and density. In order to investigate the in-medium *modification* of the cross section we also define an average free cross section $\langle\sigma_{\rm free}\rangle$, having the same structure as Eq. (9), but with the in-medium cross section $\sigma_{NN}(k,P,\rho,T)$ replaced by the free cross section $\sigma_{\rm free}(k)$.

In Fig. 2 we display the average cross sections calculated according to this procedure using the in-medium T matrix. In the upper panel of Fig. 2 we show $\langle\sigma\rangle$ as a function of p_1 for several values of density and temperature. Generally, one observes an overall reduction of the in-medium cross section compared to the free one (thin lines). As discussed more detailed in [12] this reduction is due to the modification of the density of states in the medium (reduction of the effective mass). In the case $T = 10$ MeV the average cross sections are strongly suppressed for low values p_1. The simple reason for this behavior is the Pauli blocking of the outgoing channel that forces the average cross sections even to zero at the Fermi momentum for zero temperature (see Ref. [12]). As soon as the temperature increases this suppression becomes less pronounced due to the gradual disappearance of the Pauli blocking below k_F.

In the lower panel of Fig. 2 the ratio of the average in-medium over the average free cross section is displayed. Regardless of the temperature the reduction of the in-medium cross section increases with increasing density since the ef-

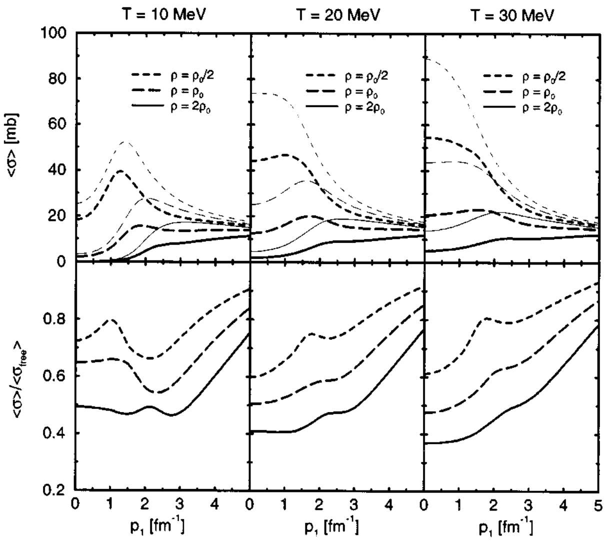

FIG. 2. Average cross section [Eq. (9)] as function of the momentum p_1 for three values of temperature and density, respectively. Upper half: absolute values of the average free (thin lines) and in-medium (thick lines) cross sections. Lower half: ratio of in-medium vs free average cross section.

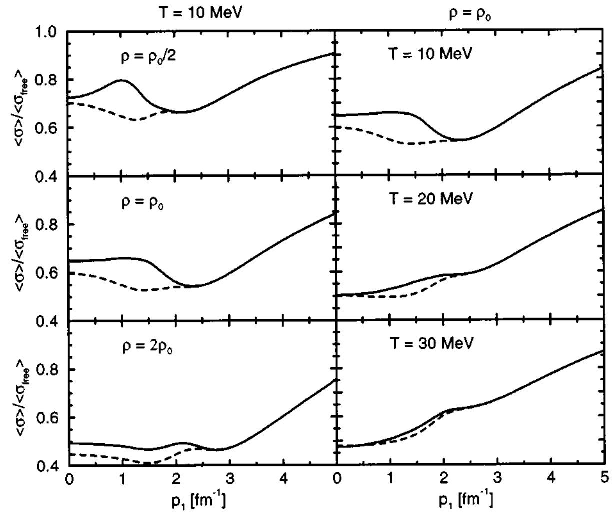

FIG. 3. Ratio of the in-medium vs free average cross section as function of the momentum p_1 calculated in G matrix (dashed lines) and T matrix (solid lines) approach. Left-hand side: fixed temperature $T=10$ MeV, three densities. Right-hand side: fixed density $\rho=\rho_0$, three temperatures.

fective mass monotonously decreases. One observes a local maximum of the ratios around the Fermi momentum that is a remnant of the critical enhancement of the in-medium cross section and loses strength with increasing density and/or temperature. The dependence on temperature of the cross section *ratios* is rather weak, in particular for large momenta $p_1 \gtrsim 2\ \mathrm{fm}^{-1}$. For smaller momenta one observes a slightly stronger suppression of the ratios with increasing temperature, due to the reduction of the critical enhancement of cross sections. We remind the reader that the origin of the temperature effects observed here is twofold: Apart from the direct temperature dependence of the in-medium scattering amplitude and density of states, the appearance of the distribution functions in the collisional integral Eq. (9) leads with varying temperature to the probing of different momentum components in the averaging procedure.

A comparison between T matrix and G matrix calculations is shown in Fig. 3, where we have plotted the ratio $\langle\sigma\rangle/\langle\sigma_{\mathrm{free}}\rangle$ as a function of p_1 both for several densities at fixed temperature $T=10$ MeV (left) and for several temperatures at fixed density $\rho=\rho_0$ (right). As an overall feature it is found that both approaches yield almost identical results beyond a certain value of the momentum which is in all cases about $p_1=2.5\ \mathrm{fm}^{-1}$. The rearrangement of the ground state associated with the hole-hole propagation is strongly suppressed for such large momenta. Furthermore, for smaller momenta the ratios calculated in the T matrix approach are larger than in the G matrix calculation due to the fact that the critical enhancement of the cross section is stronger with the T matrix. Far beyond the critical temperature of the pairing singularity the difference vanishes. However, the persistence of a deviation as large as about 10% even at densities above the saturation density could indicate that hole-hole correlations are not completely negligible in the early stage of a HIC.

Comparing the G matrix calculation here with the zero-temperature calculation of Ref. [12] one finds that the effect of finite temperature is quite considerable for momenta p_1 close to the Fermi surface, where the pronounced maximum of the ratios present in the zero-temperature case is almost completely smoothed out already at $T=10$ MeV temperature. This is connected to the rapid disappearance of the local enhancement of the effective mass with increasing temperature.

In Fig. 4 we show the ratio $\langle\sigma\rangle/\langle\sigma_{\mathrm{free}}\rangle$ as a function of the density ρ ($\rho_0/10 \leqslant \rho \leqslant 2\rho_0$) for several values of the scattering energy $E=p_1^2/2m$ in the range 100 MeV$\leqslant E \leqslant$400 MeV. All curves show a smooth and monotonic behavior. However, at the lowest temperature (10 MeV) the $E=100$ MeV curve is much less steep for densities beyond ρ_0. This is a consequence of the nonmonotonic behavior of the ratios

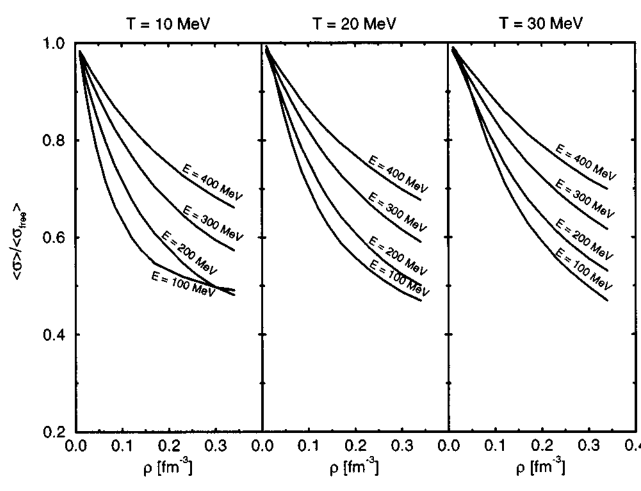

FIG. 4. Ratio of the in-medium vs free average cross section as function of the density ρ for three different temperatures and several values of the scattering energy E.

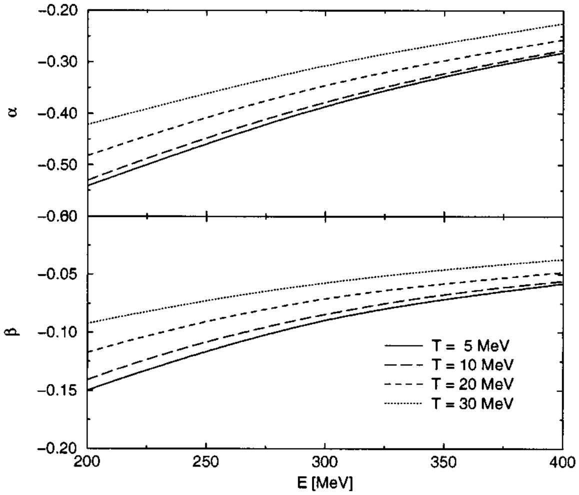

FIG. 5. Coefficients α and β for the quadratic parametrization of the density dependence of the ratio in-medium vs free average cross section as function of the scattering energy E according to Eq. (10). The figure shows the results at the four temperatures $T=5$, 10, 20, and 30 MeV.

in the low-energy range at low temperature (see Fig. 2) and leads to a crossing of the $E=100$ MeV curve with the $E=200$ MeV curve.

Because of this fact, we use for the *parametrization* of the ratios only the energy interval 200 MeV$\leqslant E \leqslant$400 MeV. The density behavior can be well described by the simple quadratic fit formula

$$\frac{\langle\sigma\rangle}{\langle\sigma_{\mathrm{free}}\rangle}(E,\rho,T)=1+\alpha(E,T)\frac{\rho}{\rho_0}-\beta(E,T)\left(\frac{\rho}{\rho_0}\right)^2,$$

$$\rho_0=0.17 \ \ \mathrm{fm}^{-3}, \qquad (10)$$

with energy- and temperature-dependent coefficients α and β. In Fig. 5 we display them as a function of the scattering energy E for several temperatures, finding a smooth and monotonic behavior. The energy dependence of α and β can be very well parametrized also by a simple quadratic fit with temperature-dependent coefficients a_i and b_i according to

$$\alpha(E,T)=a_0(T)+a_1(T)\frac{E}{E_0}+a_2(T)\left(\frac{E}{E_0}\right)^2, \qquad (11a)$$

TABLE I. Coefficients of the quadratic parametrization of α and β according to Eq. (11). The fit was done in the energy range 200 MeV$\leqslant E \leqslant$400 MeV.

T (MeV)	a_0	a_1	a_2	b_0	b_1	b_2
5	−0.997	0.554	−0.098	−0.351	0.256	−0.055
10	−0.986	0.558	−0.102	−0.337	0.252	−0.056
20	−0.890	0.501	−0.092	−0.277	0.206	−0.046
30	−0.742	0.383	−0.062	−0.206	0.142	−0.029

TABLE II. Coefficients of the temperature parametrization of a_i and b_i according to Eq. (12). The parametrization is valid in the range 5 MeV$\leqslant T \leqslant$30 MeV.

i	a_{i0}	a_{i1}	a_{i2}	b_{i0}	b_{i1}	b_{i2}
0	−1.0026	−0.0112	0.0328	−0.3674	0.0240	0.0100
1	0.5390	0.0505	−0.0342	0.2617	−0.0003	−0.0132
2	−0.0899	−0.0222	0.0105	−0.0539	−0.0055	0.0046

$$\beta(E,T)=b_0(T)+b_1(T)\frac{E}{E_0}+b_1(T)\left(\frac{E}{E_0}\right)^2, \qquad (11b)$$

$$E_0=200 \ \ \mathrm{MeV}.$$

The coefficients for the temperatures $T=5$, 10, 20, and 30 MeV are listed in Table I. In order to provide a complete parametrization we employ again a quadratic fit formula for the temperature dependence of a_i and b_i. According to the formulas

$$a_i(T)=a_{i0}+a_{i1}\frac{T}{T_0}+a_{i2}\left(\frac{T}{T_0}\right)^2, \qquad (12a)$$

$$b_i(T)=b_{i0}+b_{i1}\frac{T}{T_0}+b_{i2}\left(\frac{T}{T_0}\right)^2, \qquad (12b)$$

$$T_0=10 \ \ \mathrm{MeV},$$

we obtain coefficient matrices a_{ij} and b_{ij} which are given in Table II. We are now able to parametrize the in-medium average cross section in the ranges $0 \leqslant \rho \leqslant 2\rho_0$, 5 MeV$\leqslant T \leqslant$30 MeV, and 200 MeV$\leqslant E \leqslant$400 MeV.

In contrast to the zero-temperature G matrix calculation of Ref. [12], where we used a linear fit for the coefficients α and β, we provide here a quadratic parametrization. Having in mind the weak temperature dependence of the ratios the results of both calculations are in good qualitative agree-

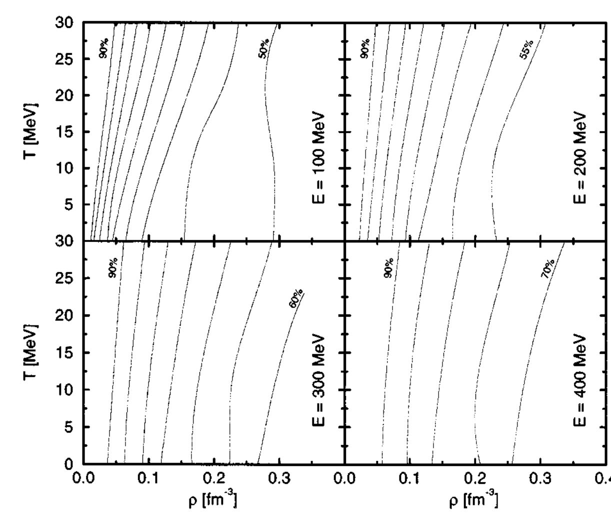

FIG. 6. Contour lines of equal ratios $\langle\sigma\rangle/\langle\sigma_{\mathrm{free}}\rangle$ in the density-temperature plane for the four values of the scattering energy $E=100$, 200, 300, and 400 MeV. The ratios are given from the highest to the lowest value in steps of 5%.

ment. However, because of the different nucleon-nucleon potentials and the difference between the G and T matrix, the present calculation does not exactly coincide with Ref. [12] in the limit $T\rightarrow 0$.

In order to obtain an overview to what extent the in-medium cross section deviates from the free one we display its behavior in the density-temperature plane in Fig. 6. This rather intuitive figure shows contours of equal ratios and thus gives an estimate for what values of temperature and density one has to account for the in-medium modification of the nucleon-nucleon cross section. Again it can be seen that the ratios depend only weakly on the temperature, particularly for large scattering energies and/or densities below normal nuclear matter density ρ_0.

In conclusion, we have determined average nucleon-nucleon cross sections that depend on the density and temperature of the nucleonic medium. The averaging procedure is suitable for application to transport-model simulations of HIC's. Convenient parametrizations of the in-medium suppression of the cross section have been given. The influence of temperature on the in-medium scattering matrix has been found to be rather small, in particular for scattering energies above about 100 MeV. For smaller energies the corresponding variations are of the order of 10%; however, this range of energies is in practice relatively unimportant due to the Pauli blocking of collisions. The inclusion of hole-hole correlations has been investigated in the T matrix approach and the resulting difference from the G matrix calculations at low temperature and scattering energy is also of the order of 10%. The results presented here were obtained with the Bonn-OBEPQ nucleon-nucleon potential, and are very close to those obtained in Ref. [12] on the basis of the Paris and Argonne V_{14} potentials, which confirms once more the insensitivity of global many-body effects, such as average in-medium cross sections, to details of the bare nucleon-nucleon interaction.

[1] J. Pochodzalla *et al.*, Phys. Rev. Lett. **75**, 1040 (1995).
[2] M. B. Tsang *et al.*, Phys. Rev. Lett. **71**, 1502 (1993); H. Xi *et al.*, GSI Report No. 97-20, 1997.
[3] W. Reisdorf *et al.*, Nucl. Phys. **A612**, 493 (1997).
[4] P. Danielewicz, in *Proceedings of the 1st International Conference on Critical Phenomena and Collective Observables, CRIS96*, Acicastello, 1996, edited by A. Insolia *et al.* (World Scientific, Singapore, 1996).
[5] G. D. Westfall *et al.*, Phys. Rev. Lett. **71**, 1986 (1993).
[6] S. Soff, S. A. Bass, C. Hartnack, H. Stöcker, and W. Greiner, Phys. Rev. C **51**, 3320 (1995).
[7] T. Alm, G. Röpke, W. Bauer, F. Daffin, and M. Schmidt, Nucl. Phys. **A587**, 815 (1995).
[8] A. Insolia, U. Lombardo, N. G. Sandulescu, and A. Bonasera, Phys. Lett. B **334**, 12 (1994).
[9] V. de la Moto, F. Sebille, M. Farine, B. Remaud, and P. Schuck, Phys. Rev. C **46**, 677 (1992).
[10] T. Izumoto, S. Krewald, and A. Faessler, Nucl. Phys. **A341**, 319 (1980); M. Trefz, A. Faessler, and W. H. Dickhoff, *ibid.* **A443**, 499 (1985); A. Bohnet, N. Ohtsuka, J. Aichelin, R. Linden, and A. Faessler, *ibid.* **A494**, 349 (1989); J. Jänicke, J. Aichelin, N. Ohtsuka, R. Linden, and A. Faessler, *ibid.* **A536**, 201 (1992); D. T. Khoa *et al.*, *ibid.* **A548**, 102 (1992); E. Lehmann, A. Faessler, J. Zipprich, R. K. Puri, and S. W. Huang, Z. Phys. A **355**, 55 (1996).
[11] M. J. Huang *et al.*, Phys. Rev. Lett. **77**, 3739 (1996).
[12] H.-J. Schulze, A. Schnell, G. Röpke, and U. Lombardo, Phys. Rev. C **55**, 3006 (1997).
[13] T. Alm, G. Röpke, A. Schnell, N. H. Kwong, and H. S. Köhler, Phys. Rev. C **53**, 2181 (1996).
[14] R. Machleidt, K. Holinde, and Ch. Elster, Phys. Rep. **149**, 1 (1987).
[15] C. Brandstaetter, diploma thesis, University of Graz, 1993 (unpublished); W. Plessas *et al.*, Few-Body Syst., Suppl. **7**, 251 (1994); H.-P. Kotz *et al.*, in *Few-Body Problems in Physics*, AIP Conf. Proc. No. 334, edited by F. Gross (AIP, New York, 1995), p. 482.
[16] G. Q. Li and R. Machleidt, Phys. Rev. C **48**, 1702 (1993); **49**, 566 (1994).
[17] M. Schmidt, G. Röpke, and H. Schulz, Ann. Phys. (N.Y.) **202**, 57 (1990); A. Sedrakian, D. Blaschke, G. Röpke, and H. Schulz, Phys. Lett. B **338**, 111 (1994); T. Alm, G. Röpke, and M. Schmidt, Phys. Rev. C **50**, 31 (1994); A. Sedrakian, G. Röpke, and T. Alm, Nucl. Phys. **A594**, 355 (1995).
[18] H.-J. Schulze, J. Cugnon, A. Lejeune, M. Baldo, and U. Lombardo, Phys. Rev. C **52**, 2785 (1995) and references therein.
[19] A. Lejeune, P. Grange, M. Martzolff, and J. Cugnon, Nucl. Phys. **A453**, 189 (1986); J. Cugnon, A. Lejeune, and P. Grange, Phys. Rev. C **35**, R861 (1987).